ELSEVIER

Nuclear Instruments and Methods in Physics Research A 464 (2001) 493–501

NUCLEAR INSTRUMENTS & METHODS IN PHYSICS RESEARCH Section A

www.elsevier.nl/locate/nima

Stabilizing influence of axial momentum spread on the two-stream instability in intense heavy ion beams

Ronald C. Davidson*, Hong Qin, Igor Kaganovich, W. Wei-li Lee

Plasma Physics Laboratory, Princeton University, Princeton, NJ 08543, USA

Abstract

This paper makes use of the Vlasov–Maxwell equations to describe the electron–ion two-stream instability driven by the directed axial motion of a high-intensity ion beam propagating through a stationary population of (unwanted) background electrons in the acceleration region or beam transport lines. The ion beam is treated as continuous in the z-direction, and the electrons are electrostatically confined in the transverse direction by the space-charge potential produced by the excess ion charge. The analysis is carried out for arbitrary beam intensity, consistent with transverse confinement of the beam particles, and arbitrary fractional charge neutralization by the background electrons. For the case of overlapping step-function ion and electron density profiles, corresponding to Kapchinskij–Vladimirskij (KV) electron and ion distributions in the transverse direction, detailed stability properties are calculated including parallel kinetic effects over a wide range of system parameters for dipole perturbations with azimuthal mode number $\ell = 1$. The instability growth rate is found to increase with increasing beam intensity, increasing fractional charge neutralization, and decreasing proximity of the conducting wall. For space-charge-dominated beams, it is shown that Landau damping associated with a modest axial momentum spread of the beam ions and background electrons has a strong stabilizing influence on the two-stream instability.

Keywords: Ion beam; Space charge; Stability; Transport

1. Introduction and theoretical model

Periodic focusing accelerators and transport systems [1–4] have a wide range of applications ranging from basic scientific research, to applications such as heavy ion fusion, spallation neutron sources, and nuclear waste transmutation. At the high beam currents and charge densities of practical interest, it is increasingly important to develop an improved theoretical understanding of the influence of the intense self-fields produced by the beam space charge and current on detailed equilibrium, stability and transport properties. For a *one-component* high-intensity beam, considerable progress has been made in describing the self-consistent evolution of the beam distribution function $f_b(\mathbf{x}, \mathbf{p}, t)$ and the self-generated electric and magnetic fields in kinetic analyses [5–9] based on the Vlasov–Maxwell equations. In many practical accelerator applications, however, an (unwanted) second charge component is present.

*Corresponding author. Fax: +1-609-243-2749.
E-mail address: rdavidson@pppl.gov (R.C. Davidson).

0168-9002/01/$ - see front matter
PII: S0168-9002(01)00117-6

For example, a background population of electrons can result by secondary emission when energetic beam ions strike the chamber wall, or through ionization of background neutral gas by the beam ions. When a second charge component is present, it has been recognized for many years, both in theoretical studies and in experimental observations [10–21], that the relative streaming motion of the high-intensity beam particles through the background charge species provides the free energy to drive the classical *two-stream* instability, appropriately modified to include the effects of DC space charge, relativistic kinematics, transverse beam dynamics, presence of a conducting wall, etc. A well-documented example is the electron–proton two-stream instability observed in the Proton Storage Ring [16–18], although a similar instability also exists for other ion species, including (for example) electron–ion interactions in electron storage rings [19–21].

In a recent theoretical calculation [10,11] that focuses on the moderate-intensity ion beams characteristic of proton linacs and storage rings, we developed a detailed kinetic description of the electron–ion two-stream instability based on the Vlasov–Maxwell equations. While that analysis [10,11] incorporated the effects of finite transverse geometry and transverse kinetic effects, it neglected the (stabilizing) influence of an axial momentum spread of the interacting charge components. In this paper, building on the techniques developed in this earlier work [10,11], we examine two-stream stability properties in the space-charge-dominated regime characteristic of heavy ion fusion, and incorporate the important effects of an axial momentum spread on detailed stability behavior.

The present analysis considers a high-intensity ion beam with distribution function $f_b(\mathbf{x},\mathbf{p},t)$, and characteristic radius r_b and average axial momentum $\gamma_b m_b \beta_b c$ propagating in the z-direction through a background population of electrons with distribution function $f_e(\mathbf{x},\mathbf{p},t)$. The ions have high directed axial velocity $V_b = \beta_b c$ in the z-direction, and the background electrons are assumed to be nonrelativistic and approximately stationary with zero average axial velocity, $\int d^3p v_z f_e \simeq 0$ in the laboratory frame. In the smooth-focusing approximation, the ion beam is assumed to be continuous in the z-direction, and the *applied* transverse focusing force on a beam ion is modeled by

$$\mathbf{F}^b_{foc} = -\gamma_b m_b \omega^2_{\beta b}(x\hat{\mathbf{x}}_x + y\hat{\mathbf{e}}_y) \tag{1}$$

where $\mathbf{x}_\perp = x\hat{\mathbf{e}}_x + y\hat{\mathbf{e}}_y$ is the transverse displacement from the beam axis, $(\gamma_b - 1)m_b c^2$ is the characteristic directed ion kinetic energy, m_b is the ion rest mass, c is the speed of light in vacuo, and $\omega_{\beta b} = \text{const.}$ is the effective betatron frequency for transverse ion motion in the applied focusing field. For the background electrons, assuming that the ion density exceeds the background electron density, the space-charge force on an electron, $\mathbf{F}^s_e = e\nabla_\perp \phi$, provides transverse confinement of the background electrons by the electrostatic space-charge potential $\phi(\mathbf{x},t)$. It is further assumed that the ion motion in the beam frame is nonrelativistic, and that the transverse momentum components of the beam ions and the characteristic spread in axial momentum are small compared with the directed axial momentum. The space-charge intensity in the present analysis is allowed to be arbitrarily large, subject only to transverse confinement of the beam ions by the focusing force in Eq. (1). Finally, the present analysis is carried out in the electrostatic and magnetostatic approximations, and the self-generated electric and magnetic fields are represented as $\mathbf{E}^s = -\nabla\phi(\mathbf{x},t)$ and $\mathbf{B}^s = \nabla A_z(\mathbf{x},t) \times \hat{\mathbf{e}}_z$, where the electrostatic potential $\phi(\mathbf{x},t)$ is determined self-consistently from Poisson's equation. Treating the axial velocity profile of the beam ions as approximately uniform over the beam cross-section, $V_{zb}(\mathbf{x},t) \simeq \beta_b c = \text{const.}$, and assuming that the electrons carry zero axial current in the laboratory frame, the z-component of vector potential $A_z(\mathbf{x},t)$ is determined self-consistently in the magnetostatic approximation from $\nabla^2 A_z = -4\pi Z_b e \beta_b n_b$. Here, $+Z_b e$ is the ion charge, and $n_b(\mathbf{x},t) = \int d^3p\, f_b(\mathbf{x},\mathbf{p},t)$ is the ion number density.

Making use of the assumptions outlined above, collective interactions between the beam ions and the background electrons are described by the nonlinear Vlasov–Maxwell equations for the ion and electron distribution functions, $f_b(\mathbf{x},\mathbf{p},t)$ and $f_e(\mathbf{x},\mathbf{p},t)$, the space-charge potential

$\phi(\mathbf{x},t)$, and the combined potential $\psi(\mathbf{x},t)=\phi(\mathbf{x},t)-\beta_b A_z(\mathbf{x},t)$. We obtain [10,11]

$$\left\{\frac{\partial}{\partial t}+\mathbf{v}\cdot\frac{\partial}{\partial \mathbf{x}}-(\gamma_b m_b\omega_{\beta b}^2\mathbf{x}_\perp+Z_b e\nabla_\perp\psi)\cdot\frac{\partial}{\partial \mathbf{p}_\perp}-Z_b e\frac{\partial\phi}{\partial z}\frac{\partial}{\partial p_z}\right\}f_b=0 \quad (2)$$

$$\left\{\frac{\partial}{\partial t}+\mathbf{v}\cdot\frac{\partial}{\partial \mathbf{x}}+e\nabla\phi\cdot\frac{\partial}{\partial \mathbf{p}}\right\}f_e=0 \quad (3)$$

$$\nabla^2\phi=-4\pi e\left(Z_b\int d^3p f_b-\int d^3p f_e\right) \quad (4)$$

$$\nabla^2\psi=-4\pi e\left(\frac{Z_b}{\gamma_b^2}\int d^3p f_b-\int d^3p f_e\right) \quad (5)$$

where $\mathbf{v}=\mathbf{p}/\gamma_b m_b$ in Eq. (2), and $\mathbf{v}=\mathbf{p}/m_e$ in Eq. (3). In Eqs. (2) and (3), we have assumed that the electrons are confined in the transverse direction by the (excess) space charge of the beam ions, and that the electrons are axially stationary in the laboratory frame with $n_e V_{ze}=\int d^3p v_z f_e\simeq 0$. As a consequence, there is no average focusing force on the electron in Eq. (3) due to the applied quadrupole focusing field, i.e., $\omega_{\beta e}=0$ is assumed.

Eqs. (2)–(5) constitute a complete description of the collective interaction of the beam ions with the background electrons based on the Vlasov–Maxwell equations. In the present analysis, we further assume that the beam propagates axially through a perfectly conducting cylindrical pipe with radius $r=r_w$. Enforcing $[E_\theta^s]_{r=r_w}=[E_z^s]_{r=r_w}=[B_r^s]_{r=r_w}=0$ readily gives $\phi(r=r_w,\theta,z,t)=0$, and $\psi(r=r_w,\theta,z,t)=0$. Here, the constant values of the potentials at $r=r_w$ have been taken equal to zero.

Finally, under *equilibrium* conditions ($\partial/\partial t=0$), the analysis assumes that ion and electron properties are spatially uniform in the z-direction with $\partial/\partial z=0$. However, the *stability* analysis assumes small-amplitude perturbations with z- and t-variations proportional to $\exp(ik_z z-i\omega t)$, where k_z is the axial wavenumber, and ω is the (complex) oscillation frequency, with $\mathrm{Im}\,\omega>0$ corresponding to instability. For present purposes, the stability analysis assumes perturbations with sufficiently long axial wavelength and high frequency that

$$k_z^2 r_b^2\ll 1 \quad (6)$$

where r_b is the characteristic beam radius. Consistent with Eq. (6), we approximate $\nabla^2\simeq\nabla_\perp^2=\partial^2/\partial x^2+\partial^2/\partial y^2$ in Eqs. (4) and (5), and neglect to leading order the contributions proportional to $(\partial/\partial z)\,\delta\phi$ in the linearized versions of Eqs. (2) and (3). Our previous investigations of the electron–ion two-stream instability [10,11] were carried out in the limit of cold beam ions and background electrons in the axial direction. An important feature of the present analysis is the incorporation of the effects of a (small) axial momentum spread on detailed stability behavior.

2. Equilibrium properties and dispersion relation

Under quasisteady equilibrium conditions with $\partial/\partial t=0$, we assume axisymmetric beam propagation ($\partial/\partial\theta=0$) and negligible variation with axial coordinate ($\partial/\partial z=0$). It is readily shown from Eqs. (2) to (5) that the equilibrium distribution functions ($\partial/\partial t=0$) for the beam ions and background electrons are of the general form

$$f_b^0(r,\mathbf{p})=F_b(H_{\perp b})G_b(p_z)$$

$$f_e^0(r,\mathbf{p})=F_e(H_{\perp b})G_e(p_z) \quad (7)$$

where $r=(x^2+y^2)^{1/2}$ is the radial distance from the beam axis, the distributions in axial momentum are normalized according to $\int_{-\infty}^{\infty}dp_z G_j(p_z)=1$, for $j=b,e$, and $H_{\perp b}$ and $H_{\perp e}$ are the single-particle Hamiltonians defined by

$$H_{\perp b}=\frac{1}{2\gamma_b m_b}\mathbf{p}_\perp^2+\frac{1}{2}\gamma_b m_b\omega_{\beta b}^2 r^2+Z_b e[\psi^0(r)-\hat{\psi}^0]$$

$$H_{\perp e}=\frac{1}{2m_e}\mathbf{p}_\perp^2-e[\phi^0(r)-\hat{\phi}^0]. \quad (8)$$

Here, for $\partial/\partial\theta=0=\partial/\partial z$, $H_{\perp b}$ and $H_{\perp e}$ are exact single-particle constants of the motion in the equilibrium field configuration, and the constants $\hat{\psi}^0\equiv\psi^0(r=0)$ and $\hat{\phi}^0\equiv\phi^0(r=0)$ are the on-axis ($r=0$) values.

There is wide latitude in specifying the functional forms of the equilibrium distribution functions [9,10]. Once $F_b(H_{\perp b})$ and $F_e(H_{\perp e})$ are specified, however, the equilibrium self-field potentials and density profiles can be calculated self-consistently from Eqs. (4) and (5) with

$\partial/\partial\theta = 0 = \partial/\partial z$. For our purposes here, we specialize to the case of electrons and ions described by the Kapchinskij–Vladimirskij (KV) distributions [1,10,11,22]

$$F_b(H_{\perp b}) = \frac{\hat{n}_b}{2\pi\gamma_b m_b}\delta(H_{\perp b} - \hat{T}_{\perp b})$$
$$F_e(H_{\perp e}) = \frac{\hat{n}_e}{2\pi m_e}\delta(H_{\perp e} - \hat{T}_{\perp e}). \quad (9)$$

In this case, it is found that the density profiles $n_j^0(r)$, $j = b, e$, correspond to overlapping step-function profiles. Here, $\hat{n}_b$ and $\hat{n}_e \equiv fZ_b\hat{n}_b$ are positive constants corresponding to the ion and electron densities, $f = \text{const.}$ is the fractional charge neutralization, and $\hat{T}_{\perp b}$ and $\hat{T}_{\perp e}$ are constants corresponding to the on-axis ($r = 0$) values of the transverse ion and electron temperatures, respectively. Without presenting algebraic details [10], some algebraic manipulation of Eqs. (4), (5), and (7)–(9) gives the step-function density profiles $n_j^0(r) = \hat{n}_j = \text{const.}$, for $0 \leqslant r < r_b$, and $n_j^0(r) = 0$ for $r_b < r \leqslant r_w$, and $j = b, e$. Here, the beam radius r_b is related to other equilibrium parameters by $\hat{\nu}_b^2 r_b^2 = 2\hat{T}_{\perp b}/\gamma_b m_b$ and $\hat{\nu}_e^2 r_b^2 = 2\hat{T}_{\perp e}/m_e$, where for monoenergetic ions and electrons, the (depressed) betatron frequencies $\hat{\nu}_b$ and $\hat{\nu}_e$ are defined by

$$\hat{\nu}_b^2 = \omega_{\beta b}^2 - \frac{1}{2}\left(\frac{1}{\gamma_b^2} - f\right)\hat{\omega}_{pb}^2 = \text{const.}$$
$$\hat{\nu}_e^2 = \frac{1}{2}\frac{\gamma_b m_b}{Z_b m_e}(1-f)\hat{\omega}_{pb}^2 = \text{const.} \quad (10)$$

where $\hat{\omega}_{pb}^2 = 4\pi\hat{n}_b Z_b^2 e^2/\gamma_b m_b$ is the ion plasma frequency squared. The inequalities, $\hat{\nu}_b^2 > 0$ and $\hat{\nu}_e^2 > 0$, are required for existence of the equilibrium.

For small-amplitude perturbations about general equilibrium distributions, $F_j(H_{\perp j})$ and $G_j(p_z)$, $j = b, e$, and corresponding self-field potentials, $\psi^0(r)$ and $\phi^0(r)$, a stability analysis proceeds by linearizing Eqs. (2)–(5). Perturbed quantities are expressed as $\delta\psi(\mathbf{x}, t) = \delta\hat{\psi}^l(r)\exp(il\theta)\exp(ik_z z - i\omega t)$, $\delta f_b(\mathbf{x}, \mathbf{p}, t) = \delta\hat{f}_b^l(r, \mathbf{p})\exp(il\theta)\exp(ik_z z - i\omega t)$, etc., where l is the azimuthal mode number, and $\text{Im}\,\omega > 0$ is assumed, corresponding to instability (temporal growth). The linearized Vlasov equations are formally integrated by using the method of characteristics [1,10,23] to integrate along the unperturbed trajectories, $\mathbf{x}'_\perp(t')$ and $\mathbf{p}'_\perp(t')$, in the equilibrium field configuration. For present purposes, we specialize to the choice of KV ion and electron distributions in Eq. (9), and the corresponding step-function equilibrium density profiles with $n_j^0(r) = \hat{n}_j = \text{const.}$, for $0 \leqslant r < r_b$, and $n_j^0(r) = 0$, for $r_b < r \leqslant r_w$. Derivation of the kinetic dispersion relation from the linearized Vlasov–Maxwell equations closely parallels the analysis in Ref. [10]. Without presenting algebraic details, for surface-wave perturbations with azimuthal mode number ℓ and axial wavenumber k_z, we obtain the dispersion relation [24]

$$\left[\frac{2}{1-(r_b/r_w)^{2\ell}} + \frac{\hat{\omega}_{pb}^2}{\ell\gamma_b^2\hat{\nu}_b^2}\Gamma_b^\ell(\omega)\right] \times \left[\frac{2}{1-(r_b/r_w)^{2\ell}} + \frac{\hat{\omega}_{pe}^2}{\ell\hat{\nu}_e^2}\Gamma_e^\ell(\omega)\right] = \frac{\hat{\omega}_{pe}^2\hat{\omega}_{pb}^2}{\ell\hat{\nu}_e^2\,\ell\hat{\nu}_b^2}\Gamma_e^\ell(\omega)\Gamma_b^\ell(\omega) \quad (11)$$

where $\hat{\omega}_{pe}^2 = 4\pi\hat{n}_e e^2/m_e$, $\hat{\omega}_{pb}^2 = 4\pi\hat{n}_b Z_b^2 e^2/\gamma_b m_b$, and $\hat{\nu}_b$ and $\hat{\nu}_e$ are the (depressed) betatron frequencies defined in Eq. (10). The ion and electron susceptibilities, $\Gamma_j^\ell(\omega)$, $j = b, e$, occurring in Eq. (11) are defined by [24]

$$\Gamma_j^\ell(\omega) = -\frac{1}{2^\ell}\sum_{m=0}^{\ell}\frac{\ell!}{m!(\ell-m)!}\int_{-\infty}^{\infty}dp_z\frac{(\ell-2m)\hat{\nu}_j G_j(p_z)}{[(\omega - k_z v_z) - (\ell-2m)\hat{\nu}_j]} \quad (12)$$

for general azimuthal mode number ℓ, and (yet unspecified) distribution in axial momentum $G_j(p_z)$. In carrying out the integration over p_z in Eq. (12), $\text{Im}\,\omega > 0$ is assumed [23,24].

Eq. (11) is the final form of the kinetic dispersion relation, derived from the linearized Vlasov–Maxwell equations for small-amplitude perturbations about the monoenergetic equilibrium distributions in Eq. (9) and the corresponding step-function density profiles. As such, Eq. (11) can be used to determine the complex oscillation frequency ω over a wide range of system parameters, including normalized beam intensity ($\hat{\omega}_{pb}^2/2\gamma_b^2\omega_{\beta b}^2$), fractional charge neutralization

($f = \hat{n}_e/Z_b\hat{n}_b$), azimuthal mode number (ℓ), axial wavenumber (k_z), choice of $G_j(p_z)$, etc., subject to the simplifying assumptions summarized earlier in this paper. In the absence of electrons ($\hat{n}_e = 0$), the dispersion relation (11) supports stable collective oscillations of the ion beam. When background electrons are present, however, Eq. (11) supports unstable solutions ($\mathrm{Im}\,\omega > 0$) with instability resulting from the axial streaming ($V_b \neq 0$) of the beam ions through the background electrons, at least in the limit where the ion and electron axial motions are 'cold' [10,11], with $G_b(p_z) = \delta(p_z - \gamma_b m_b V_b)$ and $G_e(p_z) = \delta(p_z)$.

The p_z-integration in Eq. (11) can be carried out for a variety of choices of $G_j(p_z)$ ranging from a shifted Maxwellian, to a step-function distribution, to a Lorentzian distribution. For analytical simplicity, we consider here the case of Lorentzian distributions with

$$G_b(p_z) = \frac{\Delta_b}{\pi[(p_z - \gamma_b m_b V_b)^2 + \Delta_b^2]}$$
$$G_e(p_z) = \frac{\Delta_e}{\pi(p_z^2 + \Delta_e^2)} \tag{13}$$

where $\Delta_j = \text{const.} > 0$ is a measure of the axial momentum spread, and p_z and v_z are related by $p_z = m_e v_z$ for the electrons, and $p_z = \gamma_b m_b v_z$ for the beam ions. Note from Eq. (13) that $V_b = \int_{-\infty}^{\infty} dp_z v_z G_b(p_z)$ and $0 = \int_{-\infty}^{\infty} dp_z v_z G_e(p_z)$, which corresponds to the beam ions streaming axially through a stationary electron background. Substituting Eq. (13) into Eq. (12) and integrating over p_z for $\mathrm{Im}\,\omega > 0$ readily gives the simple expression

$$\Gamma_j^\ell(\omega) = -\frac{1}{2^\ell}\sum_{m=0}^{\ell}\frac{\ell!}{m!(\ell-m)!} \times \frac{(\ell-2m)\hat{\nu}_j}{[(\omega - k_z V_j + i|k_z|v_{Tjz}) - (\ell-2m)\hat{\nu}_j]}. \tag{14}$$

Here, $V_e = 0$ for the electrons, and v_{Tjz} is a measure of the characteristic axial thermal speed, defined by $v_{Tbz} = \Delta_b/\gamma_b m_b$ for the beam ions, and $v_{Tez} = \Delta_e/m_e$ for the background electrons. Substituting Eq. (14) into Eq. (11), the resulting dispersion relation can be used to investigate the effects of an axial momentum spread on detailed properties of the electron–ion two-stream instability for general azimuthal mode number ℓ over a wide range of system parameters.

3. Dipole-mode stability properties

A careful examination of Eq. (11) for $\hat{n}_e \neq 0$ shows that the strongest instability (largest growth rate) occurs for azimuthal mode number $\ell = 1$, corresponding to a simple (dipole) displacement of the beam ions and the background electrons. For $\ell = 1$, we substitute Eq. (14) into Eq. (11), and introduce the electron and ion collective oscillation frequencies, ω_e and ω_b, defined by

$$\omega_e^2 \equiv \hat{\nu}_e^2 + \frac{1}{2}\hat{\omega}_{pe}^2\left(1 - \frac{r_b^2}{r_w^2}\right) = \frac{1}{2}\frac{\gamma_b m_b}{Z_b m_e}\hat{\omega}_{pb}^2\left(1 - f\frac{r_b^2}{r_w^2}\right)$$

$$\omega_b^2 \equiv \hat{\nu}_b^2 + \frac{\hat{\omega}_{pb}^2}{2\gamma_b^2}\left(1 - \frac{r_b^2}{r_w^2}\right) = \omega_{\beta b}^2 + \frac{1}{2}\hat{\omega}_{pb}^2\left(f - \frac{1}{\gamma_b^2}\frac{r_b^2}{r_w^2}\right) \tag{15}$$

where $\hat{\omega}_{pe}^2$ has been expressed as $\hat{\omega}_{pe}^2 = (\gamma_b m_b/Z_b m_e) f \hat{\omega}_{pb}^2$. Substituting into Eq. (11) and rearranging terms, the $\ell = 1$ dispersion relation can be expressed in the compact form [24]

$$[(\omega - k_z V_b + i|k_z|v_{Tbz})^2 - \omega_b^2] \times [(\omega + i|k_z|v_{Tez})^2 - \omega_e^2] = \omega_f^4 \tag{16}$$

where ω_f is defined by

$$\omega_f^4 \equiv \frac{1}{4} f\left(1 - \frac{r_b^2}{r_w^2}\right)^2 \frac{\gamma_b m_b}{Z_b m_e}\hat{\omega}_{pb}^4. \tag{17}$$

In the cold limit ($v_{Tbz} = 0 = v_{Tez}$), and in the absence of background electrons ($f = 0$ and $\omega_f = 0$), Eq. (16) gives stable collective oscillations of the ion beam with frequency $\omega - k_z V_b = \pm\omega_b$, where ω_b is defined in Eq. (15). For $f \neq 0$, however, the ion and electron terms on the left-hand side of Eq. (16) are coupled by the ω_f^4 term on the right-hand side, leading to one unstable

solution with $\mathrm{Im}\,\omega > 0$ for a certain range of axial wavenumber k_z. The instability is two stream in nature, and results from the directed ion motion with axial velocity V_b through the (stationary) background electrons. A careful examination of Eq. (16) shows that the unstable, positive-frequency branch has frequency and wavenumber (ω, k_z) closely tuned to the values (ω_0, k_{z0}) defined by $\omega_0 = +\omega_e$ and $\omega_0 - k_{z0}V_b = -\omega_b$, or equivalently, $k_{z0} = (\omega_e + \omega_b)/V_b$. This gives

$$\frac{\omega_0}{k_{z0}} - V_b \simeq -\frac{\omega_b}{\omega_e + \omega_b} V_b. \tag{18}$$

Because $\omega_b \ll \omega_e$ in the regimes of practical interest [Eq. (15)], it follows from Eq. (18) that the phase velocity of the unstable mode is downshifted only slightly from the directed beam velocity V_b, and could be strongly affected by Landau damping by the beam ions for modest values of $v_{Tbz}/V_b \neq 0$. As reported previously [10], the instability growth rate tends to increase with increasing fractional charge neutralization (f), and increasing values of r_w/r_b.

Returning to the full dispersion relation (16) for $v_{Tjz} \neq 0$, it is important to recognize that Eq. (16) is applicable over a wide range of beam intensity and fractional charge neutralization consistent with $\hat{\nu}_b^2 > 0$ and $\hat{\nu}_e^2 > 0$. That is, Eq. (16) can be applied to the emittance-dominated, moderate-intensity ion beams ($\hat{\omega}_{pb}^2/2\gamma_b^2\omega_{\beta b}^2 \lesssim 0.1$, say) in the proton linacs and storage rings envisioned for the Spallation Neutron Source and the Proton Storage Ring [16–18]. On the other hand, Eq. (16) can also be applied to the low-emittance, very high-intensity ion beams envisioned for heavy ion fusion [4].

At the high beam intensities of interest for heavy ion fusion, the transverse beam emittance (which is proportional to $\hat{T}_{\perp b}$) is very low, and the normalized beam intensity $\hat{\omega}_{pb}^2/2\gamma_b^2\omega_{\beta b}^2$ can approach unity in the absence of background electrons ($f = 0$). This follows from the inequality $\hat{\nu}_b^2/\omega_{\beta b}^2 = 2\hat{T}_{\perp b}/\gamma_b m_b \omega_{\beta b}^2 r_b^2 \ll 1$ and the definition of $\hat{\nu}_b^2$ in Eq. (10). At such high beam intensities, it is necessary to solve the full dispersion relation (16) for the complex oscillation frequency ω. Typical results are illustrated in Fig. 1 (for $v_{Tbz} = 0 = v_{Tez}$)

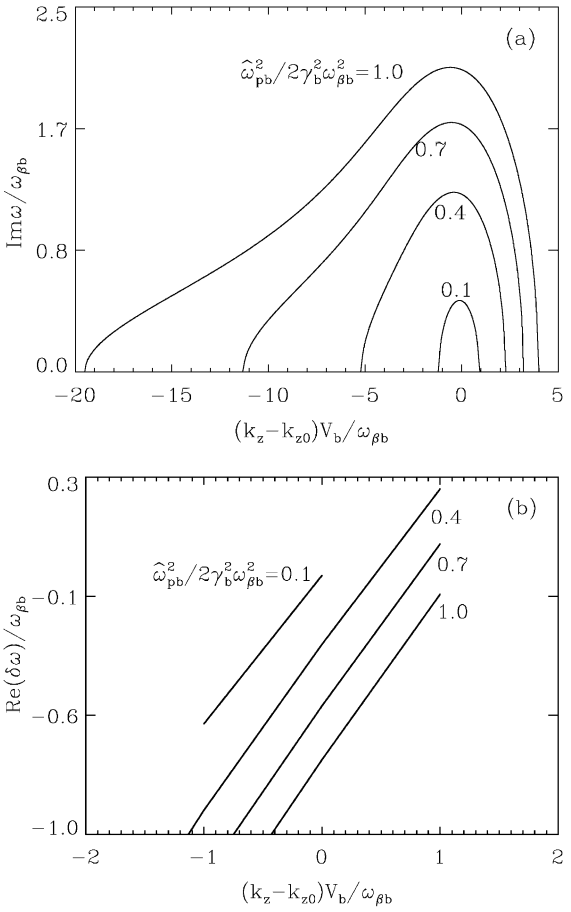

Fig. 1. Plots of (a) normalized growth rate $\mathrm{Im}\,\omega/\omega_{\beta b}$, and (b) normalized real frequency $(\mathrm{Re}\,\omega - \omega_e)/\omega_{\beta b}$ versus shifted axial wavenumber $(k_z - k_{z0})V_b/\omega_{\beta b}$ obtained from the dispersion relation (16) for the unstable branch with positive real frequency. System parameters correspond to $v_{Tbz} = 0 = v_{Tez}$, $Z_b = 1$, $A = 133$ (Cesium ions), $(\gamma_b - 1)m_b c^2 = 4.5$ GeV, $r_b/r_w = 0.5$, and $f = 0.1$. Curves are shown for several values of normalized beam intensity $\hat{\omega}_{pb}^2/2\gamma_b^2\omega_{\beta b}^2$ ranging from 0.1 to 1.0.

and in Fig. 2 (for $v_{Tbz} \neq 0$, and $v_{Tez} = v_{Tbz}$). The system parameters in Figs. 1 and 2 correspond to $Z_b = 1$, $A = 133$ (Cesium ions), $(\gamma_b - 1)m_b c^2 = 4.5$ GeV, $r_b/r_w = 0.5$, and $f = 0.1$.

Shown in Fig. 1, for $v_{Tbz} = 0 = v_{Tez}$, are plots of $(\mathrm{Im}\,\omega)/\omega_{\beta b}$ and $(\mathrm{Re}\,\omega - \omega_e)/\omega_{\beta b}$ versus $(k_z - k_{z0})V_b/\omega_{\beta b}$, where $k_{z0} \equiv (\omega_e + \omega_b)/V_b$, obtained from Eq. (16) for the unstable branch for several values of $\hat{\omega}_{pb}^2/2\gamma_b^2\omega_{\beta b}^2$ ranging from

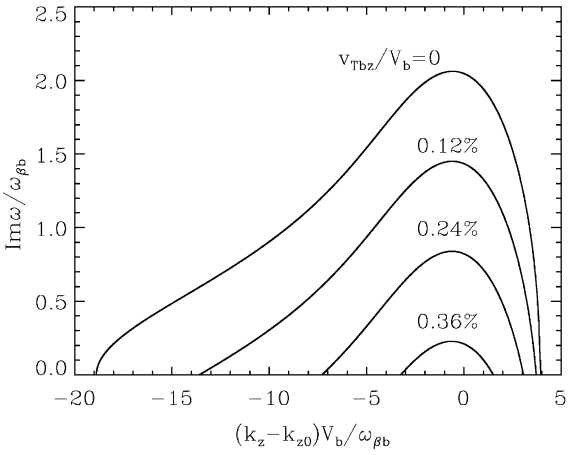

Fig. 2. Plots of (a) normalized growth rate $\mathrm{Im}\,\omega/\omega_{\beta b}$, and normalized real frequency $(\mathrm{Re}\,\delta\omega)/\omega_{\beta b}$ versus shifted axial wavenumber $(k_z - k_{z0})V_b/\omega_{\beta b}$ obtained from Eq. (16) for the unstable branch with positive real frequency. Here, $\delta\omega = \omega - \omega_e$. System parameters correspond to $\hat{\omega}_{pb}^2/2\gamma_b^2\omega_{\beta b}^2 = 0.98$, $v_{Tez} = v_{Tbz}$, $Z_b = 1$, $A = 133$ (Cesium ions), $(\gamma_b - 1)m_b c^2 = 4.5$ GeV, $r_b/r_w = 0.5$, and $f = 0.1$. Curves are shown for several values of normalized ion thermal spread v_{Tbz}/V_b ranging from 0% to 0.36%.

0.1 to 1.0. At low beam intensities, the instability growth rate in Fig. 1 is relatively small and has a narrow bandwidth in k_z-space, symmetric about $k_z = k_{z0}$. On the other hand, as the normalized beam intensity $\hat{\omega}_{pb}^2/2\gamma_b^2\omega_{\beta b}^2$ is increased to values approaching unity, the instability bandwidth increases significantly in Fig. 1, and the growth rate becomes substantial, with $(\mathrm{Im}\,\omega)_{max} \simeq 2.1\omega_{\beta b}$.

To illustrate the stabilizing influence of parallel kinetic effects on the two-stream instability, shown in Fig. 2 are plots of $(\mathrm{Im}\,\omega)/\omega_{\beta b}$ and $(\mathrm{Re}\,\omega - \omega_e)/\omega_{\beta b}$ versus $(k_z - k_{z0})/\omega_{\beta b}$, obtained from Eq. (16) for the unstable branch for fixed value of the normalized beam intensity, $\hat{\omega}_{pb}^2/2\gamma_b^2\omega_{pb}^2 = 0.98$, and values of v_{Tbz}/V_b ranging from 0% to 0.36%. Furthermore, for purposes of illustration in Fig. 2 we have fixed the axial momentum spread of the electrons by the value $v_{Tez} = v_{Tbz}$. Because the characteristic phase velocity of the unstable mode is downshifted only slightly from the directed beam velocity V_b [Eq. (18)], it is expected that Landau damping by parallel kinetic effects can have a strong stabilizing influence at modest values of v_{Tbz}/V_b. That this is indeed the case is evident from Fig. 2, which shows a substantial reduction in maximum growth rate and eradication of the instability over the instability bandwidth as v_{Tzb}/V_b is increased from 0% to 0.36%.

The dispersion relation (16) can be used to derive an analytical criterion for stabilization of the two-stream instability by parallel kinetic effects, valid for normailized beam intensity $s_b = \hat{\omega}_{pb}^2/2\gamma_b^2\omega_{\beta b}^2$ ranging from moderate values ($s_b < 0.1$) of interest in proton machines, to the space-charge dominated beams ($s_b \to 1$) of interest in heavy ion fusion. It is convienient to express $\delta\omega = \omega - \omega_e$ and $\delta k_z = k_z - k_{z0}$, where $k_{z0} = (\omega_e + \omega_b)/V_b$, ω_e and ω_b are defined in Eq. (15). Because $|\delta\omega| \ll \omega_e$ [see Figs. 1 and 2, and Eq. (15)] in the regimes of practical interest, it follows that the dispersion relation (16) can be approximated by the cubic equation for $\delta\omega$,

$$(\delta\omega + i|k_z|v_{Tbz} - \delta k_z V_b)(\delta\omega + i|k_z|v_{Tez}) \times [1 - (2\omega_b)^{-1}(\delta\omega + i|k_z|v_{Tbz} - \delta k_z V_b)] = -\frac{\omega_f^4}{4\omega_e\omega_b}. \quad (19)$$

In analyzing Eq. (19), it is convenient to introduce the dimensionless parameters, Γ_0^2 and α, defined by

$$\Gamma_0^2 \equiv \frac{\omega_f^4}{16\omega_e\omega_b^3}$$

$$\alpha \equiv \left[1 + \frac{27}{2}\Gamma_0^2 + 3\sqrt{3}\Gamma_0\left(1 + \frac{27}{4}\Gamma_0^2\right)^{1/2}\right]^{1/3}. \quad (20)$$

For purpose of illustration, we further consider the case where $v_{Tez} = v_{Tbz}$. From Figs. 1 and 2, it is clear that the maximum growth rate occurs for $\delta k_z = 0$ and $v_{Tbz} = v_{Tez} = 0$. Furthermore, as v_{Tjz} is increased, it is clear from Fig. 2 that the maximum growth rate is reduced, and that the instability is completely stabilized over the entire spectrum when the axial momentum spread exceeds some critical value. We set $\delta k_z = 0$ and $v_{Tez} = v_{Tbz}$ in Eq. (19), and solve for the growth rate $\gamma = \mathrm{Im}\,\delta\omega$ of the unstable mode ($\mathrm{Im}\,\delta\omega > 0$)

as a function of increasing $v_{\mathrm{Tb}z}/V_{\mathrm{b}}$. Denoting $\Delta p_{z\mathrm{b}}/\gamma_{\mathrm{b}} m_{\mathrm{b}} V_{\mathrm{b}} = v_{\mathrm{Tb}z}/V_{\mathrm{b}}$, where $\Delta p_{z\mathrm{b}} = \Delta_{\mathrm{b}}$ is the axial momentum spread [Eq. (13)], we find that the two-stream instability is completely stabilized ($\mathrm{Im}\,\delta\omega \leqslant 0$) provided the axial momentum spread is sufficiently large that

$$\frac{\Delta p_{z\mathrm{b}}}{\gamma_{\mathrm{b}} m_{\mathrm{b}} V_{\mathrm{b}}} > \frac{1}{\sqrt{3}\omega_{\mathrm{e}} + \omega_{\mathrm{b}}} \left| \alpha - \frac{1}{\alpha} \right| \equiv \left(\frac{\Delta p_{z\mathrm{b}}}{\gamma_{\mathrm{b}} m_{\mathrm{b}} V_{\mathrm{b}}} \right)_{\mathrm{cr}} . \tag{21}$$

In the regimes of practical interest for heavy ion fusion, the right-hand side of Eq. (21) is very small, and only modest momentum spreads are required to provide complete stabilization of the two-stream instability.

Making use of the definitions of $\omega_{\mathrm{b}}, \omega_{\mathrm{e}}, \omega_f$ and α in Eqs. (15), (17) and (20) the stability criterion in Eq. (21) can be applied over a wide range of system parameters. As illustrative conditions for heavy ion fusion, we take $Z_{\mathrm{b}} = 1$, $A = 133$ (Cesium ions), $(\gamma_{\mathrm{b}} - 1) m_{\mathrm{b}} c^2 = 4.5$ GeV, $r_{\mathrm{b}}/r = 0.5$, and $f = 0.1$. Shown in Fig. 3 is the corresponding plot of $(\Delta p_{z\mathrm{b}}/\gamma_{\mathrm{b}} m_{\mathrm{b}} V_{\mathrm{b}})_{\mathrm{cr}}$ versus normalized beam intensity, $s_{\mathrm{b}} = \hat{\omega}_{\mathrm{pb}}^2/2\gamma_{\mathrm{b}}^2 \omega_{\beta\mathrm{b}}^2$, for s_{b} in the interval $0 < s_{\mathrm{b}} \leqslant 1$. Although the momentum spread required for stabilization increases as s_{b} is increased, it is clear from Fig. 3 that only a relatively modest spread $(\Delta p_{z\mathrm{b}}/\gamma_{\mathrm{b}} m_{\mathrm{b}} V_{\mathrm{b}})_{\mathrm{cr}}$ is required for complete stabilization in the space-charge-dominated regime with $s_{\mathrm{b}} \to 1$. Furthermore, from Eqs. (20) and (21), at fixed value of s_{b}, the value of $\Delta p_{z\mathrm{b}}/\gamma_{\mathrm{b}} m_{\mathrm{b}} V_{\mathrm{b}}$ required for stabilization decreases as the fractional charge neutralization f is decreased.

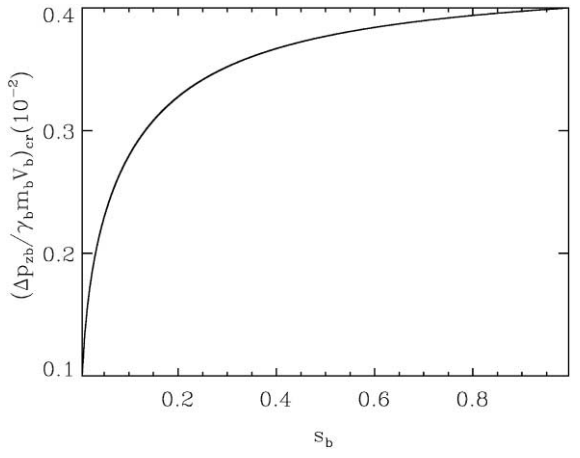

Fig. 3. Plot of $(\Delta p_{z\mathrm{b}}/\gamma_{\mathrm{b}} m_{\mathrm{b}} V_{\mathrm{b}})_{\mathrm{cr}}$ versus normalized beam intensity $s_{\mathrm{b}} = \hat{\omega}_{\mathrm{pb}}^2/2\gamma_{\mathrm{b}}^2 \omega_{\beta\mathrm{b}}^2$ obtained from Eq. (21) for $Z_{\mathrm{b}} = 1$, $A = 133$ (Cesium ions), $(\gamma_{\mathrm{b}} - 1) m_{\mathrm{b}} c^2 = 4.5$ GeV, $r_{\mathrm{b}}/r_{\mathrm{w}} = 0.5$ and $f = 0.1$. Here, $\omega_{\mathrm{e}}, \omega_{\mathrm{b}}, \omega_f$ and α are defined in Eqs. (15), (17) and (20).

4. Conclusions

For $k_z^2 r_{\mathrm{b}}^2 \ll 1$, the dispersion relation (11) incorporates the leading-order effects of an axial momentum spread in the ion and electron components, and can be used to investigate detailed stability properties over a wide range of normalized beam intensity ($\hat{\omega}_{\mathrm{pb}}^2/2\gamma_{\mathrm{b}}^2\omega_{\beta\mathrm{b}}^2$), fractional charge neutralization ($f = \hat{n}_{\mathrm{e}}/Z_{\mathrm{b}}\hat{n}_{\mathrm{b}}$), azimuthal mode number (ℓ), and axial wavenumber (k_z). For dipole perturbations ($\ell = 1$), it has been shown that Landau damping by parallel kinetic effects can have a strong stabilizing influence on the electron–ion two-stream instability. The condition for complete stabilization of the electron–ion two-stream instability by parallel kinetic effects is given by Eq. (21) for the case where $v_{\mathrm{Te}z} = v_{\mathrm{Tb}z}$. The inequality in Eq. (21) corresponds to a relatively small axial momentum spread at the very high beam intensities of interests for heavy ion fusion (see Fig. 3), where $s_{\mathrm{b}} = \hat{\omega}_{\mathrm{pb}}^2/2\gamma_{\mathrm{b}}^2\omega_{\beta\mathrm{b}}^2 \to 1$. It should also be emphasized that the present linear stability analysis is carried out for surface-wave perturbations, focusing on dipole-mode perturbations ($l = 1$). For the particular choice of KV distribution functions in Eq. (9), body-mode perturbations with radial node structure $n = 1, 2, 3, \ldots$, may also exhibit instability [1,5], depending on the value of $l = 0, 1, 2, \ldots$, and the normalized beam intensity s_{b}.

Finally, if the beam ions and background electrons are initially cold axially, it is expected that a nonlinear consequence of the two-stream instability would be to cause an increase in axial momentum spread to a value comparable to Eq. (21), thereby leading to a (quasilinear) stabilization of the instability.

Acknowledgements

This research was supported by the US Department of Energy, and the Short-Pulse Spallation Source project and LANSCE Division of the Los Alamos National Laboratory, and the Spallation Neutron Source project.

References

[1] R.C. Davidson, Physics of Nonneutral Plasmas, Addison-Wesley Publishing Co., Reading, MA, 1990, and references therein.
[2] M. Reiser, Theory and Design of Charged Particle Beams, John Wiley & Sons, Inc., New York, 1994.
[3] T.P. Wangler, Principles of RF Linear Accelerators, John Wiley & Sons, Inc., New York, 1998.
[4] See, for example, in: I. Hofmann (Ed.), Proceedings of the 1997 International Symposium on Heavy Ion Inertial Fusion, Nucl. Instr. and Meth. Phys. Res. 415 (1998) 1–508, and references therein.
[5] T.-S. Wang, L. Smith, Part. Accel. 12 (1982) 247.
[6] J. Struckmeier, I. Hofmann, Part. Accel. 39 (1992) 219.
[7] R.C. Davidson, Phys. Plasmas 5 (1998) 3459.
[8] R.C. Davidson, Phys. Rev. Lett. 81 (1998) 991.
[9] R.C. Davidson, C. Chen, Part. Accel. 59 (1998) 175.
[10] R.C. Davidson, H. Qin, P.H. Stoltz, T.-S. Wang, Phys. Rev. Special Topics Accel. Beams 2 (1999) 054 401, and references therein.
[11] R.C. Davidson, H. Qin, T.-S. Wang, Phys. Lett. A 252 (1999) 213.
[12] H. Qin, R.C. Davidson, W.W. Lee, Am. Inst. Conf. Proc. 496 (1999) 295.
[13] D.G. Koshkarev, P.R. Zenkevich, Part. Accel. 3 (1972) 1.
[14] E. Keil, B. Zotter, CERN Report CERN-ISR-TH/71-58 1971.
[15] L.J. Laslett, A.M. Sessler, D. Möhl, Nucl. Instr. and Meth. Phys. Res. 121 (1974) 517.
[16] D. Neuffer, E. Colton, D. Fitzgerald, T. Hardek, R. Hutson, R. Macek, M. Plum, H. Thiessen, T.-S. Wang, Nucl. Instr. and Meth. Phys. Res. A 321 (1992) 1.
[17] D. Neuffer, C. Ohmori, Nucl. Instr. and Meth. Phys. Res. A 343 (1994) 390.
[18] M.A. Plum, D.H. Fitzgerald, D. Johnson, J. Langenbrunner, R.J. Macek, F. Merrill, P. Morton, B. Prichard, O. Sander, M. Shulze, H.A. Thiessen, T.-S. Wang, C.A. Wilkinson, Proceedings of the 1997 Particle Accelerator Conference, Vol. 1611, 1997.
[19] M. Izawa, Y. Sato, T. Toyomasu, Phys. Rev. Lett. 74 (1995) 5044.
[20] J. Byrd, A. Chao, S. Heifets, M. Minty, T.O. Raubenheimer, J. Seeman, G. Stupakov, J. Thomson, F. Zimmerman, Phys. Rev. Lett. 79 (1997) 79.
[21] K. Ohmi, Phys. Rev. E 55 (1997) 7550.
[22] I. Kapchinskij, V. Vladimirskij, in: Proceedings of the International Conference on High Energy Accelerators and Instrumentation, CERN Scientific Information Service, Geneva, 1959, p. 274.
[23] See, for example, R.C. Davidson, Physics of Nonneutral Plasmas, Addison-WesleyPublishing Co., Reading, MA, 1990 (Chapters 2, 4, and 10).
[24] R.C. Davidson, H. Qin, Effects of axial momentum spread on the electron–ion two-stream instability in high-intensity ion beams, Phys. Lett. A 270 (2000) 177.